Simultaneous Retrieval of Surface Roughness Parameters from Combined Active-Passive Microwave Observations

Anke Fluhrer, *Member, IEEE,* Thomas Jagdhuber, *Senior Member, IEEE*, Ruzbeh Akbar, *Member, IEEE*, Peggy O'Neill, *Fellow, IEEE*, Dara Entekhabi, *Fellow, IEEE*

***Abstract*— An active-passive microwave retrieval algorithm for simultaneous determination of soil surface roughness parameters (vertical RMS height (s) and horizontal correlation length (l)) is presented for bare soils. The algorithm is based on active-passive microwave covariation including the improved Integral Equation Method (I^2EM) and is tested with global SMAP observations. Estimated retrieval results for s and l are overall consistent with values in the literature, indicating the validity of the proposed algorithm. Sensitivity analyses showed that the developed roughness retrieval algorithm is independent of permittivity for $\varepsilon_s > 10$ [-]. Furthermore, the physical model basis of this approach (I^2EM) allows application of different autocorrelation functions (ACF), such as Gaussian and exponential ACFs. Global roughness retrieval results confirm bare areas in deserts such as Sahara or Gobi. However, the type of ACF used within roughness parameter estimation is important. Retrieval results for the Gaussian ACF describe a rougher surface than retrieval results for the exponential ACF. No correlations were found between roughness results and the amount of precipitation or the sand and clay fractions, which could be due to the coarse spatial resolution of the SMAP data. The extension of this approach to vegetated soils is planned as an add-on study.**

***Index Terms*— correlation length, I^2EM, radar, radiometer, RMS height, SMAP**

I. INTRODUCTION

A. *Motivation for surface roughness estimation*

The estimation and monitoring of geophysical parameters via earth-observation satellites is crucial for improving our understanding of global environmental and hydrological processes. Soil roughness is an essential parameter in physical processes related to water, energy, and nutrient flow and exchange, since it characterizes the boundary between the pedosphere and atmosphere [1]. Soil roughness influences microwave signals from soil surfaces and contributes to measurements from active as well as passive sensors. Both radar backscatter $|S_{PP}|^2$ [dB] and microwave emission E_P [-], based on brightness temperature TB_P [K], are sensitive to surface roughness. While $|S_{PP}|^2$ is mostly dominated by soil moisture and soil surface roughness, TB_P is a function of soil moisture, soil surface roughness and the effective surface temperature over bare soils [2], [3].

Despite its importance for environmental applications, soil roughness has played a minor role in land parameter retrieval with microwave remote sensing in recent decades [4], [5]. For instance, soil roughness is an important parameter in land surface modeling of soil erosion applications, because it defines the soil surfaces that represent "the interface between the eroding soil body and the erosive agent" [6], [1], [3], [5].

Retrieval of geophysical parameters such as soil roughness or soil moisture is mainly performed at lower frequencies, like at L-band (1.4 GHz). Lower frequencies are typically used due to the high sensitivity of active and passive microwave L-band signatures to soil moisture (under vegetation). Moreover, C-band (~ 6 GHz) and higher frequency bands are less applied because of the reduced sensitivity of higher microwave frequencies to underlying soil moisture and soil roughness as vegetation canopies become denser [3], [7], [8]. Further, the operational monitoring of soil moisture content on global scales has been mainly performed continuously with passive microwave sensors. Passive microwave sensors are used predominantly since soil roughness and vegetation hold a stronger influence on backscatter than on soil-emitted brightness temperature [9].

The primary disadvantage of passive-only retrievals is the coarse spatial resolution of microwave radiometers in orbit (> 40 km), which is sufficient for large-scale applications, such as global climate modelling. Yet, for weather forecasting and agricultural yield management, soil moisture information of at least 10 km spatial resolution is desired [10]. Active microwave sensors provide a higher spatial resolution than passive microwave sensors. Unfortunately, studies in recent years have shown that estimations of geophysical parameters on the basis of radar-only retrievals are prone to errors. This might be due to two reasons: Firstly, there are difficulties in quantifying all occurring scattering effects [9], [11-13], and secondly, the impact of terrain and vegetation morphology are often not considered adequately in radar retrievals due to their complex structures [9]. Thus, the combination of both active and passive sensor systems can improve monitoring of geophysical parameters, such as soil surface roughness, by leveraging the advantages of both sensors while overcoming their individual limitations.

Currently, the existing soil moisture retrieval algorithms for a joint processing of radar and radiometer microwave satellite data are the change detection method [7], [14], [15] and the Soil Moisture Active Passive (SMAP) optional [10] and the SMAP baseline [10], [16] downscaling algorithms. In all of these algorithms soil roughness is considered only as a secondary effect. Therefore, soil roughness is corrected either by collecting multi-configuration data (variety of frequency and/or polarization) or by optimizing it within the parameter retrieval algorithm until the model predictions coincided with the actual measured data. However, Saatchi *et al.* noted that for a precise monitoring of soil moisture, accurate determination of surface roughness is key to correctly deriving soil moisture information from radar data [17].

B. *Parameterization of Surface Roughness in Remote Sensing*

The two fundamental parameters describing soil surface roughness are the standard deviation of the surface height variation (or vertical RMS height), with its related autocorrelation function (ACF), and the horizontal correlation length [8]. Due to the non-standardized naming convention, the terminology for both parameters is ambiguous. Common parameterizations for the vertical RMS height are S_D, σ or s [4], [8], [18], [19], and for the horizontal correlation length L_C or l

Manuscript received ; revised ; accepted . Date of publication . *(Corresponding author: Anke Fluhrer.)*

This work was supported in part by the MIT-Germany Seed Fund "Global Water Cycle and Environmental Monitoring using Active and Passive Satellite-based Microwave Instruments."

A. Fluhrer and T. Jagdhuber are with the German Aerospace Center, Microwaves and Radar Institute, Muenchener Strasse 20, 82234 Weßling, Germany (e-mail: Anke.Fluhrer@dlr.de). A. Fluhrer is with the University of Augsburg, Institute of Geography, Alter Postweg 118, 86159 Augsburg.

R. Akbar and D. Entekhabi are with the Department of Civil and Environmental Engineering, Massachusetts Institute of Technology, Cambridge, MA 02139 USA.

P. E. O'Neill is with the NASA Goddard Space Flight Center, Greenbelt, MD 20771 USA.

[2], [20]. In this study, the standard deviation of the surface height variation is denoted by s [cm], with its related ACF [-], and the horizontal correlation length by l [cm], which is the naming convention already used, e.g., in [1], [8], [21], [22].

For the sake of completeness, it should be mentioned that passive microwave retrievals often refer to a different roughness parameter. They are using a radiative transfer model to simulate effects of surface roughness on measured brightness temperature TB_P [4]. This model is the analytical zero-order solution to the Radiative Transfer equation, commonly referred to as the tau-omega ($\tau - \omega$) model [23], or the L-band Microwave Emission of the Biosphere (L-MEB) model [19]. Within these models, soil emission is calculated based on a semi-empirical approach first proposed by Wang & Choudhury 1981 [24], known as HQN [20] or $H - Q$ model [25]. Wang & Choudhury [24] pointed out that the Fresnel equations can be used to describe the reflectivity of a smooth but not a rough soil surface. In the latter case, scattering of the incident wave occurs in many directions and the reflected parts "in the specular direction would be lower than the Fresnel reflectivity" [24]. To account for this fact, the soil roughness loss factor, $h = H_R \cdot cos^N\theta$, was introduced [4] to consider reflectivity losses caused by increasing surface roughness. Here, a different roughness parameter, called H_R [19], is used to characterize roughness effects on passive microwave signatures.

In this study, we determine the vertical RMS height and the horizontal correlation length of a surface, and can link h with s by $H_R = (2 \cdot s \cdot k)^2$, where k [cm^{-1}] is the wave number ($k = 2\pi/\lambda$) [4], [18], [19], [26]. In the HQN model, the parameter Q is called the polarization mixing factor which accounts for differences in values between the horizontal and the vertical polarization. Lastly, within the HQN model to describe the reflectivity of a rough surface, the parameter N accounts for multi-angular and dual-polarization measurements which is set equal to two in most studies [20], [24].

In addition to s and l, a third roughness parameter is important for some surface models, such as the improved Integral Enhanced Method (I^{2}EM). This parameter is called the roughness slope m, which can be calculated by $m = s/l$. The slope m should in general for L-band be lower than 0.3 [8] or 0.4 [27] in case of single scattering and bare soil surfaces with moderate RMS heights [28].

When remotely sensing soil surfaces, the roughness of one surface always depends on the wavelength of the observation system. Hence, s and l are estimated in wavelength units and have to be scaled by the wave number k to the units of meters. Because of this wavelength dependence, it is important at which scale surface roughness is observed. Depending on the wavelength and the incidence angle of the microwave sensor, it can be observed at small, medium or large scale. In general, with decreasing wavelength or increasing incidence angle, roughness is observed at smaller scales. In the field of microwave remote sensing, surface roughness is mainly observed at centimeter scale, since "[a]t microwave frequencies, the wavelength is on the order of centimeters to a few tens of centimeters" [8].

The objective of this study is to simultaneously determine the vertical (s) and horizontal (l) components of soil surface roughness through the combination of active and passive microwave data.

C. Advantage of Active and Passive Microwave Signature Combination

As an example of how the joint use of radar and radiometer can improve soil moisture estimations, Fig. 1 shows overlays of radar-only and radiometer-only cost functions along permittivity ε_s and roughness parameter s.

Similar to Akbar *et al.* the computed backscatter $\Delta\,|S_{PP}|^2$ (radar-only) and emission $\Delta\,E_P$ (radiometer-only) spaces are displayed for a vector of unknowns ($\bar{x} = [\varepsilon_s, s, l]$) [29]. ε_s ranges from 2.6 to 50 in 0.1 steps, s values from 0.05 cm to 10 cm, and l values from 1 cm to 21 cm, each in 0.1 cm steps. In Fig. 1, we assume $l = 14$ cm and plot $\Delta\,|S_{PP}|^2 < 30$ dB and $\Delta\,E_P < 0.01\,[-]$ to emphasize model predictions in the vicinity of the true test point (red circle), which is the global minimum of the cost function. The results for the horizontal polarization (cf. Fig. 1A) and the vertical polarization (cf. Fig. 1B) are shown individually since "scattering polarization behaviors are different" [29].

It can be understood from Fig. 1 that the possible range of valid permittivity values that yield $\Delta\,|S_{PP}|^2 \cong 0$ extend over the entire range of initial ε_s values. This holds true for both polarizations. The possible range of values for s spans from 1.2 cm to 5 cm. In the case of the radiometer, the possible range of permittivity values is slightly reduced and extends from 14 to 50 for the horizontal polarization (cf. Fig. 1A) and from 14 to 30 for the vertical polarization (cf. Fig. 1B). However, the range of possible values for s now covers the entire range of initial s values (from 0.05 cm to 5 cm). Therefore, if only radars or radiometers are used, it is not clear which pairs (ε_s, s) lead to most accurate estimates. This disadvantage is further amplified by the presence of measurement noise.

By combining radar- and radiometer-only cost functions, the search space for optimum parameter values is significantly reduced, since the complementary physics of backscatter and emission limits the possible parameter search space. Consequently, lower retrieval errors can be achieved compared to retrievals only based on one sensor. The combined approach effectively reduces the susceptibility of radars to permittivity and the susceptibility of radiometers to roughness.

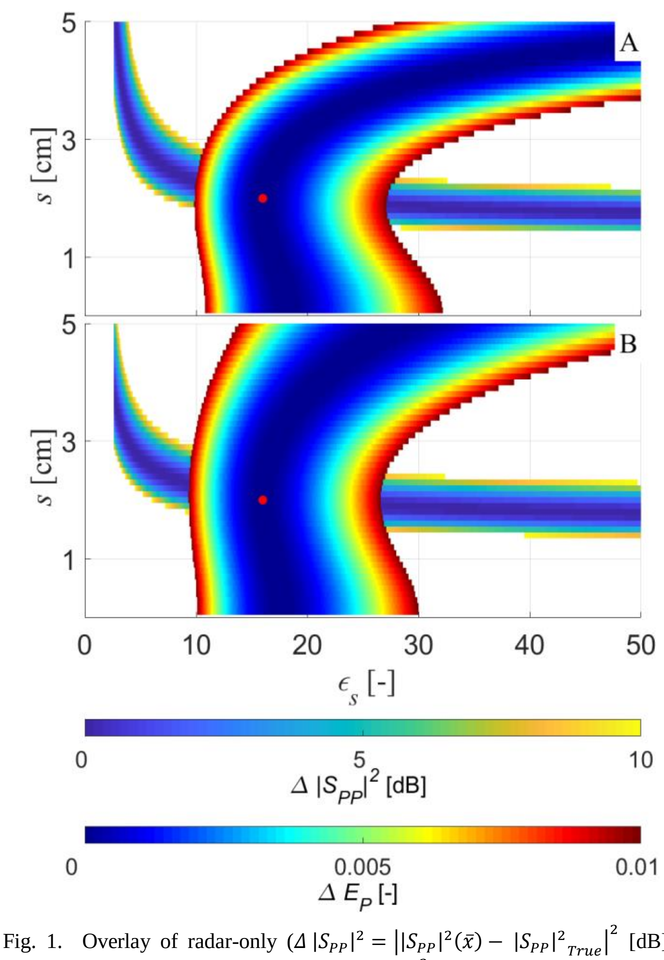

Fig. 1. Overlay of radar-only ($\Delta\,|S_{PP}|^2 = \left||S_{PP}|^2(\bar{x}) - |S_{PP}|^2{}_{True}\right|^2$ [dB]) and radiometer-only ($\Delta\,E_P = |E_P(\bar{x}) - E_{P_{True}}|^2$ [-]) cost functions modelled with I^{2}EM assuming a Gaussian ACF: (A) Overlay for horizontal polarization, (B) Overlay for vertical polarization. Red circles are the true test point (global minimum) at input parameters $\varepsilon_s = 15\,[-]$, $s = 2\,cm$ and $l = 14\,cm$. Study similar to Akbar *et al.*, 2017 [29].

II. DATA

Data for this study come from the NASA SMAP mission [3]. This mission was launched in 2015 with the aim to exploit synergies between active and passive instruments at L-band frequency. It is the first soil moisture dedicated space-borne mission developed to provide moisture products from active and passive microwave satellite data [3], [30]. Unfortunately, the SMAP radar went out of service in July 2015 after only three months of operations, but the SMAP radiometer continues to deliver high-quality data [29]. Due to the radar failure, the investigation period with SMAP data in this study is limited to the period from 14th of April until 7th of July 2015.

The data used in this study are the SMAP L1B Radar Half-Orbit Time-Ordered low resolution backscatter $|S_{PP}|^2$ [31], the SMAP L1C Radiometer Half-Orbit Time-Ordered Brightness Temperatures TB_P [32], the physical soil temperature T_S and soil moisture obtained from the SMAP L3SM_P products [33], all posted on a 36 km Equal-Area Scalable Earth-2 (EASE-2) grid [34], [35].

In order to guarantee analyses exclusively over bare soils we filter the global surface roughness results for vegetation, water or snow. We used the vegetation optical depth (VOD) posted on a 36 km EASE-2 grid from the SMAP dataset processed with the multi-temporal dual-channel retrieval algorithm (MT-DCA) [35], and the surface condition quality flags for snow and frozen ground from the SMAP L3 Radiometer Global and Northern Hemisphere Daily 36 km EASE-Grid Freeze/Thaw State [36] for filtering. Pixels with VOD greater than 0.06, with more than one day covered by snow or frozen ground during the investigation period, or with more than 5% water fraction are masked out.

III. METHODS

Simultaneous acquisition of radar ($|S_{HH}|^2$ and $|S_{VV}|^2$) and radiometer (TB_H and TB_V) measurements allows concurrent estimation of up to three unknown parameters – roughness parameters s, l and permittivity ε_s (cf. sec. I.A.).

In this bare surface study, we concurrently determine s and l by first relating backscatter and emission through the p-polarized smooth surface reflectivity term r_P [23], [37]. This specific linkage enables isolating r_P as a function of permittivity ε_s.

Soil emission can be written as function of a roughness loss term, $f_e(s,l)$, and r_P [23], [37]:

$$E_P = 1 - f_e(s,l) \cdot r_P(\varepsilon_s). \tag{1}$$

Likewise, the total surface backscatter can be expressed as the product of another roughness loss term $f_s(s,l)$ and r_P [38]:

$$|S_{PP}|^2 = f_s(s,l) \cdot r_P(\varepsilon_s). \tag{2}$$

By isolating the smooth surface reflectivity term $r_P(\varepsilon_s)$ in (1) and (2), we can link emission with backscatter in the absence of vegetation through active-passive microwave covariation β_{P-PP} [38]:

$$\frac{f_e(s,l)}{f_s(s,l)} = \frac{E_P - 1}{|S_{PP}|^2} = \frac{TB_P/T_S - 1}{|S_{PP}|^2} = \beta_{P-PP}(s,l), \tag{3}$$

where T_S is the surface physical temperature within the top 5 cm of the soil [2].

In (3) β_{P-PP} is referred to as the covariation parameter, for respective polarization P. The specific form of (3) allows us to calculate β_{P-PP} based on physical models of bare surface backscatter and emission, β_{P-PP}^{Model} [-]. Coincidentally, β_{P-PP} can also be calculated from quasi-simultaneously acquired active and passive microwave measurements, henceforth β_{P-PP}^{Data}. The only limiting factor is that both sensors (radar and radiometer) must have the same spatial resolution in order to observe roughness at the same scale.

For surface roughness estimation, we calculate β_{P-PP}^{Model} and β_{P-PP}^{Data} based on simulated and data-based backscatter and emission, respectively. Then, we minimize the absolute difference between model prediction β_{P-PP}^{Model} and the calculated observations-driven β_{P-PP}^{Data} for s and l estimation. To ensure valid roughness estimation, we used the roughness slope with $m < 0.3$ as a threshold (cf. sec. I.B.). This condition is also used as validity criterion for the Small Perturbation Model (SPM) [8] which is embedded in I^{2}EM when L-band frequency is applied. The details for modelled and data-based covariation parameters are as follows.

A. *Model-based Retrieval of Active-Passive Microwave Covariation*

β_{P-PP}^{Model} is calculated by forward simulations of surface emission (E_P) and backscatter ($|S_{PP}|^2$) using (3). To proceed, we first defined a valid range of values for $s \in [0, 5]$ cm in 0.25 cm steps, and $l \in [1, 40]$ cm in 1.0 cm steps. The third input parameter is soil permittivity and ranges from $\varepsilon_s \in [2, 50]$ in 1.0 steps. Furthermore, s and l are calculated using both Gaussian and Exponential ACFs.

In this study we simulate backscatter and emission values with the I^{2}EM to calculate β_{P-PP}^{Model} [8]. The reason for employing the I^{2}EM is its physical basis for backscatter and emission based on s and l, frequency f, incident angle θ and permittivity ε_s [8], [39], [40]. Because of its analytical formulation, I^{2}EM is preferred over computationally more expensive numerical methods, such as the Numerical Maxwell Model in 3-D (NMM3D) [41].

B. *Data-based Retrieval of Active-Passive Microwave Covariation*

The covariation parameter, calculated with SMAP data inserted in (3), is called data-based covariation parameter β_{P-PP}^{Data} [-]. In this study, β_{P-PP}^{Data} , is calculated based on SMAP observations specified in section II.

IV. SENSITIVITY ANALYSIS

As mentioned above, we eliminate the smooth surface reflectivity term as a function of permittivity ε_s in order to solve for two unknowns at the same time, the surface roughness parameters s and l. ε_s is hence only an input variable for the simulations of backscatter and emission. In order to evaluate the permittivity dependence of our proposed covariation-based retrieval algorithm, we compared the full range of physically reasonable ε_s-values with the estimated model-based covariation parameter β_{P-PP}^{Model}, computed with NMM3D as well as I^{2}EM (cf. sec. III.A.). As shown in Fig. 2, β_{P-PP}^{Model} remains nearly constant over the entire range of permittivity values for both employed models except for small permittivity values. β_{P-PP}^{Model} changes only for ε_s lower than approx. ten, representing arid and hyper-arid soils. The reason for this is found in the formulation of covariation with emission over backscatter (cf. (3), sec. III.). The backscatter falls exponentially to very low values for these small permittivity values, which in turn causes larger dynamics in covariation. However, for $\varepsilon_s > 10$ β_{P-PP}^{Model} is insensitive to permittivity dynamics. Consequently, the retrieval algorithm is independent of permittivity variations in case of non-arid soils.

V. RESULTS

This section presents the roughness results obtained from SMAP observations using the proposed covariation-based active-passive algorithm (cf. (3), sec. III.). Additionally, the results for varying ACFs are compared and analyzed in the context of changing weather and soil conditions.

A. *Results of Surface Roughness Parameter Estimation*

In the following, the retrieval results for the roughness parameters s and l are presented. Note that the proposed approach only applies to

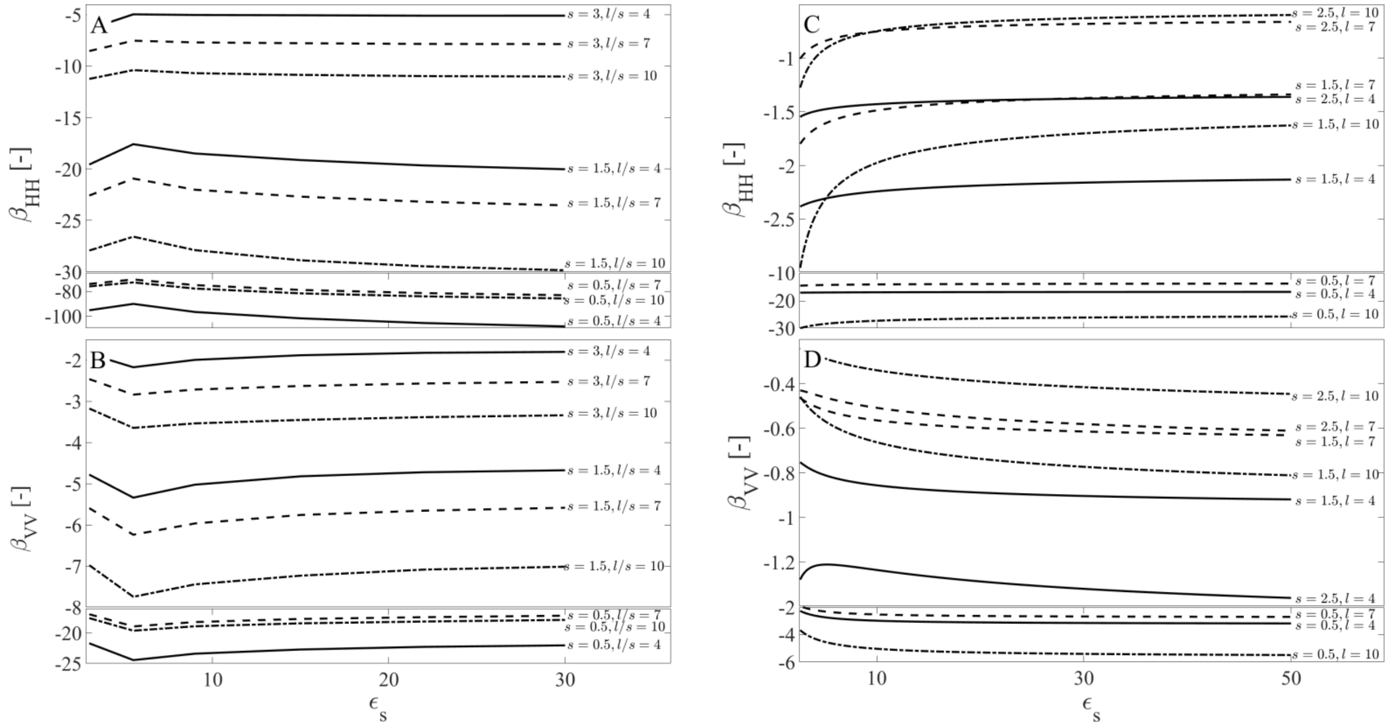

Fig. 2. Influence of soil permittivity ε_s on covariation parameter β_{P-PP}^{Model} modelled with NMM3D or I²EM assuming a Gaussian ACF, s of 0.5 cm, 1.5 cm and 3 cm and the ratio l/s of 4 cm, 7 cm and 10 cm. (A) NMM3D results for β_{H-HH}^{Model}, (B) NMM3D results for β_{V-VV}^{Model}, (C) I²EM results for β_{H-HH}^{Model}, (D) I²EM results for β_{V-VV}^{Model}. The y-axes are interrupted since β_{P-PP}^{Model} increases to large negative values for very smooth surfaces.

bare surfaces. These regions are located almost exclusively in North Africa, Asia or Australia. For reasons of better readability, we will therefore only display results for this sub-region.

Figure 3 illustrates the median of estimated s and l for the sub-region Africa-Asia-Australia, which were calculated assuming a Gaussian ACF. The results for s are between 0.35 cm and 7 cm, with a majority of the values (~72.3%) between 0.35 cm and 2.5 cm. The lowest values for s are found within the Sahara, and the highest values at the edges of deserts (e.g. Sahara, Gobi) or in the Arabian Peninsula due to increasing vegetation cover (e.g. shrublands) or rocks (cf. Fig. 3A). The results for l range between 1.75 cm and 20.5 cm, with correlation lengths mostly (~86.4%) of 6 cm to 16 cm. The lowest values for l are estimated, for example, in the Sahara or in the southern part of Australia. The highest values for l are found in the northwestern part of Australia as well as in Kazakhstan and Mongolia (cf. Fig. 3B).

Comparing the roughness estimates calculated assuming either a Gaussian (cf. Fig. 3) or an exponential ACF (cf. Fig. 4), the roughness patterns for the two ACFs generally appear similar. However, results for the Gaussian ACF are higher for s and lower for l compared to the results for the exponential ACF. About 72.3% of all s values assuming a Gaussian ACF are between 0.35 cm and 2.5 cm, whereas over 82.2% of all s values are located in the same range when assuming an exponential ACF. In addition, over 86.4% of values for l are located between 6 cm to 16 cm for the Gaussian ACF, but only 60.2% are located in that same range for the exponential ACF, since overall larger l values are retrieved (cf. Fig. 4).

In summary, comparisons between both types of ACFs for the retrieved s values show overall smaller s in case of an exponential ACF (cf. Figs. 3A, 4A). For l it is the other way round, since correlation lengths are lower if a Gaussian ACF is assumed (cf. Figs. 3B, 4B).

Based on estimated roughness results for s and with $N = 2$ (cf. sec. I.B.), the roughness loss factor h is calculated assuming a Gaussian ACF (cf. Fig. 5A) or an exponential ACF (cf. Fig. 5B). The values for h are in the range between 0 and 2. As can be seen in Fig. 5, assuming a Gaussian ACF, the majority of values (~79.7%) are located between 0 and 1.5 with a peak between 0.6 and 0.7 (cf. inset of Fig. 5A).

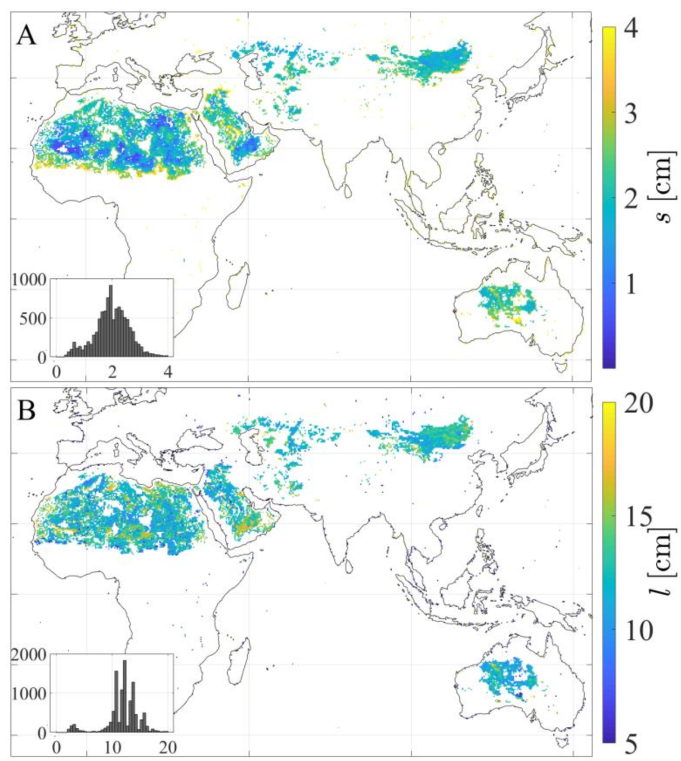

Fig. 3. Temporal median (April-July 2015) of estimated surface roughness parameters s and l from SMAP observations for the sub-region Africa-Asia-Australia assuming a Gaussian ACF. (A) Vertical RMS height s, (B) Horizontal correlation length l.

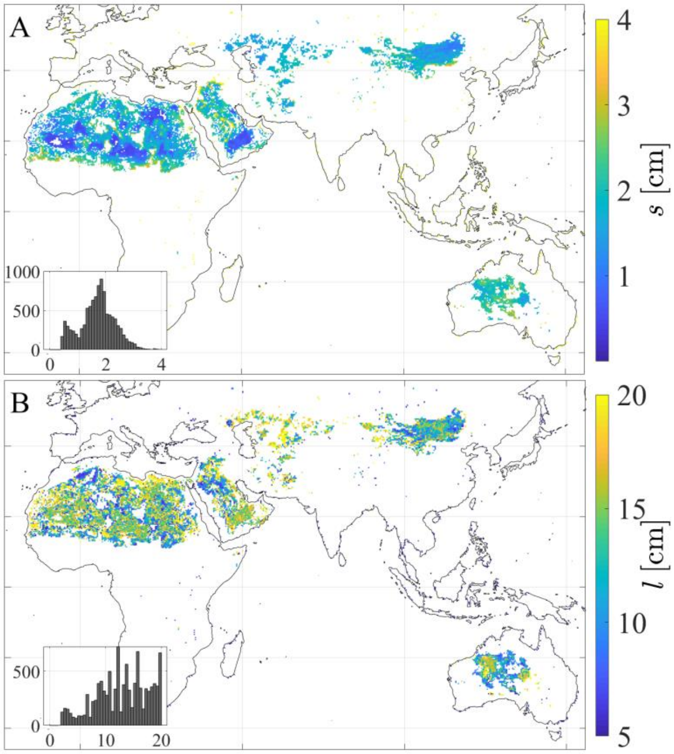

Fig. 4. Temporal median (April-July 2015) of estimated surface roughness parameters s and l from SMAP observations for the sub-region Africa-Asia-Australia assuming an exponential ACF. (A) Vertical RMS height s, (B) Horizontal correlation length l.

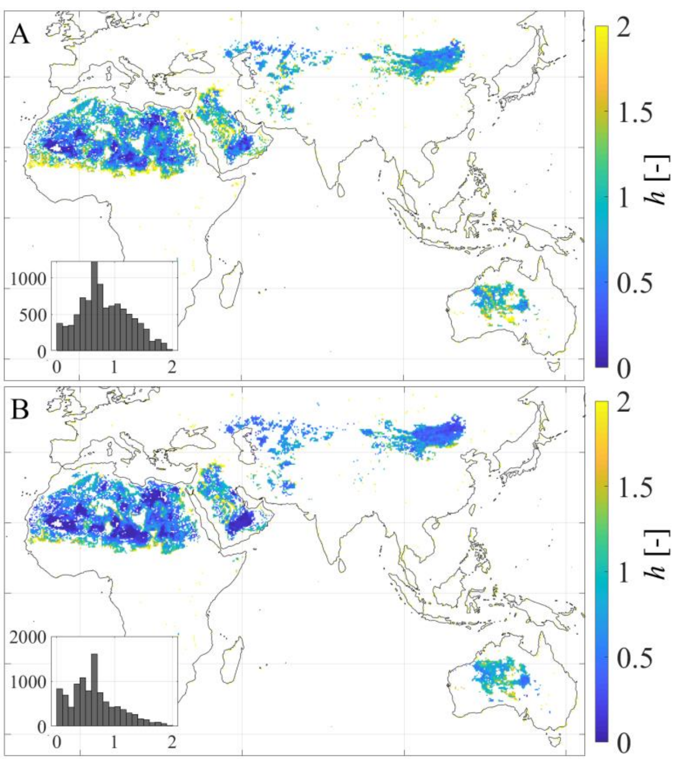

Fig. 5. Temporal median (April-July 2015) of estimated roughness loss factor h for the sub-region Africa-Asia-Australia based on surface roughness parameters s from SMAP observations. (A) Gaussian ACF, (B) Exponential ACF.

In case of an exponential ACF, approx. 86.1% of all values for h are located in the range between 0 and 1.5. However, its peak is also between 0.6 and 0.7, whereas the magnitude is dropping significantly towards higher values. Hence, overall lower values for h are obtained assuming an exponential instead of a Gaussian ACF. By definition, the spatial patterns of h are equivalent to the ones of s (cf. Fig. 3-5).

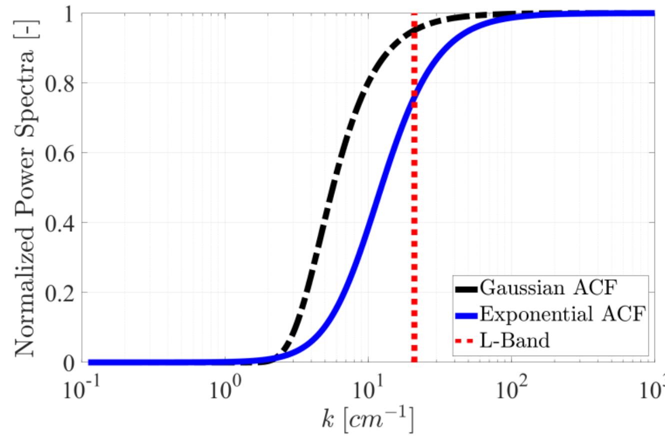

Fig. 6. Comparison of the normalized power spectra [-] for the Gaussian (black line) and exponential (blue dashdot line) autocorrelation functions (ACF) at L-band (red dashed line) along wave number k [cm^{-1}], calculated based on (9) and (10) of [42].

For a more detailed investigation of the differences between the results of both ACFs, we analyzed their power spectra, as described in [42]. Defined as "a measure of the amplitude of each Fourier component scattered by a rough surface" [43], the power spectrum explains the surface type assumed for the ACF. We calculated the respective power spectrum for both ACFs along different wave numbers according to [42] and normalized them by their respective amplitude to allow direct comparisons.

Fig. 6 shows the normalized power spectra of both ACFs and the case for L-band ($\lambda = 21$ cm) as a red dashed line. The roughness values calculated with an exponential ACF stay below the level of the values calculated with Gaussian ACF. Hence, the Gaussian ACF describes a rougher soil surface, whereas the exponential ACF describes a smoother soil surface at L-band, according to presented retrieval results displayed in Fig. 3 and 4.

B. Comparison of Surface Roughness Estimates with Precipitation and Soil Conditions

Analyses are performed to investigate possible correlations between estimated roughness parameters and external factors such as weather or soil conditions.

We used data from the Yanco Agricultural Institute, Bureau of Meteorology, Australia [44] to investigate the influence of precipitation on soil surface roughness.

In Fig. 7 we compare the daily *in situ* precipitation measurements and the corresponding SMAP soil moisture [33] values with roughness retrieval results at the Yanco test site, Australia. It can be seen that soil moisture and precipitation follow each other and correlate, as expected. However, both show no correlation with the SMAP-based results for s and l, regardless the type of ACF (cf. Fig. 7). This lack of correlation between roughness results and precipitation was also tested between roughness and soil moisture for the entire sub-region Africa-Asia-Australia (not shown here). Analysis of temporal correlation between the change of estimated roughness parameters s and l and the SMAP soil moisture dynamics show no significant correlation, whereby the most frequent value in the analyzed histograms is zero with a standard deviation of 0.14.

In addition, the estimated roughness patterns were compared with VOD from SMAP MT-DCA retrievals [35] and sand or clay fractions of soils from [45], both posted on the 36 km EASE-2 grid.

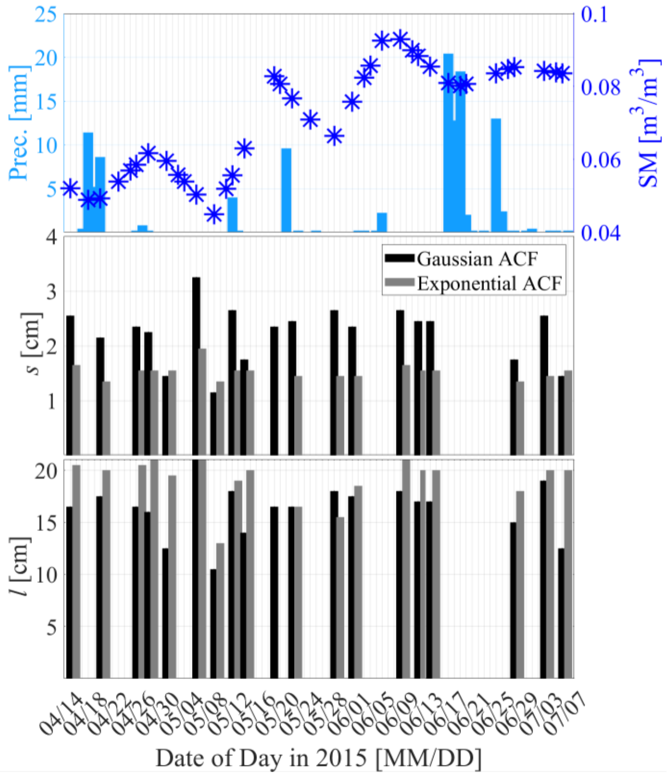

Fig. 7. Daily precipitation measurements from the Yanco agricultural institute, Bureau of Meteorology, Australia [44] (bright blue bars) and soil moisture from SMAP [33] (dark blue stars) in comparison with retrieval results for surface roughness parameters s and l, based on SMAP observations, assuming a Gaussian ACF (black bars) or exponential ACF (gray bars), at the Yanco weather station (NSW, 34.60°S, 146.42°E).

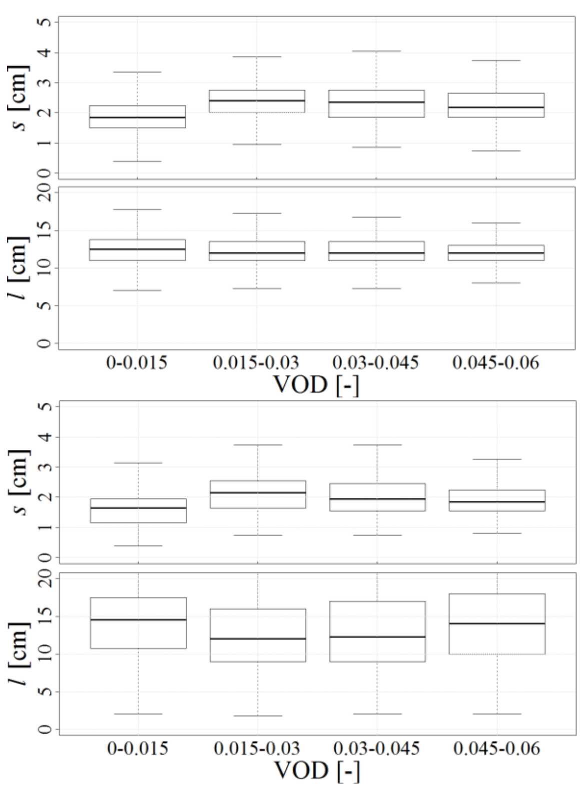

Fig. 8. Comparison of estimated surface roughness parameters s and l with vegetation optical depth (VOD) [-] [35], both from SMAP observations for the sub-region Africa-Asia-Australia. (A) Gaussian ACF, (B) Exponential ACF.

Fig. 8 shows that retrieval results for s are slightly increasing until VOD class 0.015 to 0.03 and then slightly decrease. In contrast, results for l are slightly decreasing until VOD class 0.015 to 0.03 and then slightly increase. Despite the overall similar distribution patterns, the value ranges for both ACFs are significantly different for roughness parameter l, with much larger ranges for the exponential ACF. However, no influence of vegetation could be observed at higher VOD values. In extended analyses up to VOD of 1.12 (not shown here), we get higher values for s and lower values for l. Reason for this is that with increasing vegetation canopy we rather get a mix of signal effects from ground (roughness) and vegetation. The value ranges of estimated s and l for all VOD classes from 0 to 0.06 thus confirm the effective filtering before estimating the surface roughness parameters (cf. Section II.).

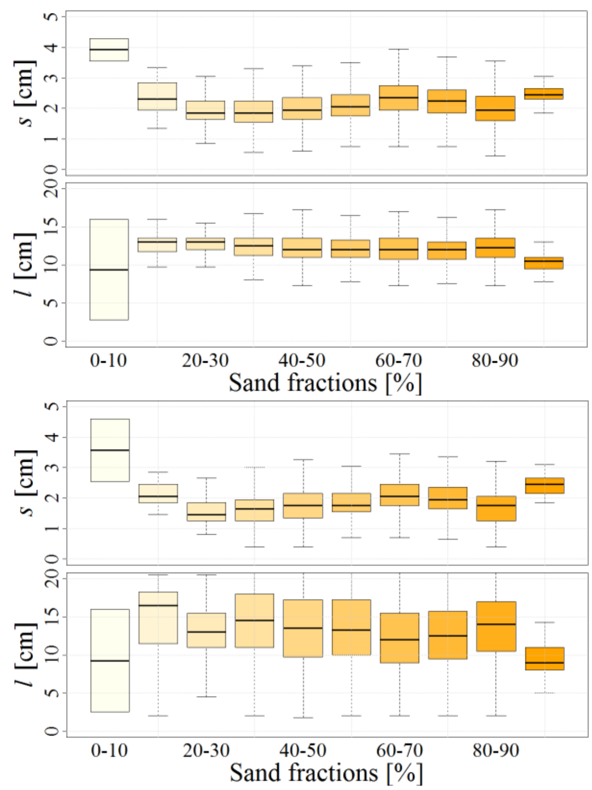

Fig. 9. Comparison of estimated surface roughness parameters s and l retrieved from SMAP observations with sand fractions from [45] for the sub-region Africa-Asia-Australia. (A) Gaussian ACF, (B) Exponential ACF.

Lastly, we compared surface roughness results with the sand and clay fractions used as ancillary data within the SMAP parameter retrievals [45]. Fig. 9 shows that the overall distribution patterns are quite similar for both employed ACFs. Similar to results displayed in Fig. 8, the value ranges are larger for the exponential ACF than for the Gaussian ACF. It can be seen that estimated s peaks for the smallest sand fraction (0-10%). On the contrary, results for estimated l are lowest for the smallest sand fraction. Additionally, the overall dynamic of l along increasing sand fractions (from 20% to 90%) is very low with absolute differences in median values of only 0.75 cm (Gaussian ACF), and 2.5 cm (exponential ACF) (cf. Fig. 9). In summary, the value ranges for s are similar for both ACFs, whereas the ranges for l assuming an exponential ACF are approximately two to three times larger than for the Gaussian ACF. However, the variation between sand fractions is reasonable and does not show a distinct correlation between roughness parameters and sand fractions. When comparing the roughness results with clay fractions (not shown here), the most significant finding is that there is no correlation between clay fractions and the soil surface roughness parameters, similar to the case for sand fractions. Another finding is that there are no estimates of s and l for clay fractions greater than 70%. The fact that no roughness results overlap with clay fractions greater than 70% is consistent with the global distribution of clay fractions from the Harmonized World Soil Database (HWSD) [46].

VI. Discussion

Our covariation-based approach requires equivalent spatial resolution for radar and radiometer acquisitions in order to observe roughness at the same scale. Most spaceborne radar sensors provide a much higher resolution than radiometer sensors. In the case of the SMAP mission, the radar had a spatial resolution of ~3 km until its failure, whereas the radiometer has a resolution of ~40 km [3]. Since our approach is limited to simultaneously acquired polarimetric active/passive microwave datasets with comparable spatial resolutions, data suitable beyond this study include the airborne PALS datasets [14], [47] or the spaceborne AQUARIUS data [48]. Despite these limitations in acquisition and resolution, our roughness retrieval technique outperforms any ground-based sensing method in terms of acquisition time and spatial coverage.

The covariation-based approach including the forward model I^{2}EM for the retrieval of s and l provides the possibility of employing varying ACFs and the simultaneous estimation of both roughness components with centimeter precision. By using the I^{2}EM we extended the valid restrictions for possible surface roughness scales compared to, for instance, the SPM, and the applicability also for a broader range of frequencies [8]. The study from [39] showed that the I^{2}EM is in good agreement with the SPM at low frequencies and with the standard Kirchhoff model (KM) at high frequency regions.

Within the proposed approach, we consider the two commonly applied ACFs of Gaussian and exponential type for characterization of the soil surface. Previous studies by [21] and [49] showed that for rather smooth bare surfaces the correlation function is close to the exponential ACF, whereas for very rough surfaces it is close to the Gaussian ACF. Especially for surface roughness of agriculturally managed soils, parameterization is more complex and variable, since the ACF is affected by the characteristics of tillage, spanning several roughness scales. Nonetheless, also for agriculturally managed soils most studies confirm an exponential ACF for smooth and Gaussian ACF for very rough surfaces (e.g. after plowing) [21], [50], [51]. Moreover, previous studies pointed out that surface roughness parameters are close to an exponential ACF when sensing over bare soils at L-Band [11], [25], [52]. Comparison of roughness results outlined the differences between both ACFs. We estimated values for s mainly in the range between 0.35 cm and 2.5 cm and for l between 6 cm to 16 cm, assuming a Gaussian ACF. For the assumption of an exponential ACF we estimated overall lower s and higher l values. Thus, the exponential ACF describes a smoother roughness pattern whereas the Gaussian ACF describes a rather rough surface roughness pattern, equivalent to literature [21], [50], [51]. Ogilvy and Foster [43] investigated in a numerical study Gaussian and exponential correlation functions of theoretically generated random rough surfaces. They found that the exponential ACF tends to correlate roughness on a fine scale due to a rapid loss of correlation. By contrast, the Gaussian ACF decreases more slowly over distance and hence tends to correlate roughness not on a very fine scale [43]. Their explanation for varying roughness correlations was found to be the shape of the respective power spectra. In the case of the exponential ACF, it is a Lorentzian transform of the correlation function, whereas in the case of the Gaussian ACF it is given by the Fourier transform of the correlation function [43]. Hence, the influence of the employed ACF type is distinct and the assumption of Zhixiong *et al.* that for homogeneous agricultural fields the ACF is unrelated to surface roughness conditions cannot be confirmed here [53].

In this study, we also presented results for the roughness loss factor h, which is the prominent parameter used in passive microwave retrievals based on the HQN-model [20], [24] (cf. sec. I.B.). Results for h are located mainly between 0 and 1.5 with most values between 0.6 and 0.7, independent of the employed type of ACF. In the literature, typical values for H_R are located between 0 and 1.7, depending on the type and amount of vegetation canopy [20]. These correspond to h values between 0 and 1 (cf. sec. I.B.). Values for H_R greater than 1 are only estimated for forests, with typical values for grass or open shrublands mostly around 0.4 [20], which equals an h value of 0.23. With our covariation-based approach, where h peaks between 0.6 and 0.7, we are apparently overestimating h since our study areas are limited to bare soils only. Nonetheless, similar studies which are estimating the single scattering albedo ω directly instead within the $\tau - \omega$ model are also retrieving higher values compared to theoretical definitions [54]. Hence, we directly retrieve s and subsequently h, with estimated roughness values for h fitting to the expected smooth to moderately rough bare surfaces.

For detailed analyses of globally retrieved roughness patterns from SMAP observations, we compared results for s and l with sand or clay fractions. From those analyses it can be understood that for our study setup the respective sand or clay fraction of a soil shows no distinct influence on s and l. However, we compared all roughness results retrieved from SMAP observations at once. This means that we do not consider different types of soils. Thus, comparisons of roughness results with individual major soil types to account for sand or clay dominated soils is needed to investigate the relation between surface roughness and specific soil types in more detail [55].

VII. Summary and Conclusions

This study presents a covariation-based active-passive microwave retrieval algorithm for simultaneous estimation of vertical and horizontal soil surface roughness components (s, l) from bare soils. Within this approach we use radar and radiometer data from both horizontal and vertical polarizations with equivalent spatial resolution to calculate the active-passive microwave covariation for each individual radar-radiometer acquisition pair (no time series needed). This way, the approach enables a simultaneous retrieval of both roughness parameters (s, l) over a larger area (compared to *in situ* measurements).

Results show that the proposed approach leads to valid retrievals of s and l, with consistencies of more than 90% between model simulations and roughness results.

By conducting a series of sensitivity tests, it was found that the influence of permittivity (soil moisture) on our covariation-based approach is only significant for arid soils with $\varepsilon_s < 10$ (cf. sec. IV).

We also tested the effectiveness of our filtering of data, in order to ensure analyses exclusively over bare soils, based on VOD values. Since no influence of vegetation could be observed at higher VOD values we concluded that the filtering prior to the estimation of roughness results for vegetation was successful.

Moreover, no significant correlation between precipitation and surface roughness parameters could be found despite the often applied assumption that soil surface roughness smoothens with precipitation. One reason could be that this assumption only applies to agricultural managed soils after tilling. Furthermore, results outline that changes in surface roughness are not correlated to changes in soil moisture. Similar to correlations between estimated roughness patterns and precipitation or soil moisture, no correlation could be found between roughness parameters and sand or clay fractions. The reason for the lack of correlations in all correlation analyses might be that we investigate global roughness patterns from SMAP observations with ~36 km spatial resolution where precipitation effects might be nondominant in the recorded signal.

Detailed investigations regarding the influence of the assumed type of ACF revealed that both Gaussian and exponential ACF describe different types of roughness patterns, and our conclusions are consistent with previous studies. Hence, the employed type of ACF for surface roughness estimation is crucial and must be considered carefully.

In summary, the retrieved roughness parameters have the potential to improve soil moisture estimates, even from satellite data and for global scales. This supports soil moisture estimation for hydrometeorology or climate research.

The proposed technique for surface roughness retrieval from combined active and passive microwave signatures is currently limited to bare soils. In order to enable the estimation under vegetated soils, our covariation-based algorithm needs to be updated for vegetation-based scattering as well as emission [38].

Acknowledgments

The authors would like to thank Mark Luetzner from DLR for the English proofreading. The authors are grateful to MIT for supporting this research with the MIT-Germany Seed Fund "Global Water Cycle and Environmental Monitoring using Active and Passive Satellite-based Microwave Instruments".

References

[1] P. Marzahn and R. Ludwig, "On the derivation of soil surface roughness from multi parametric PolSAR data and its potential for hydrological modeling," in *Hydrol. Earth Syst. Sci*., 13, 381-394, 2009, DOI: 10.5194/hess-13-381-2009.

[2] P. K. Srivastava, P. O'Neill, M. Cosh, M. Kurum, R. Lang and A. Joseph, "Evaluation of Dielectric Mixing Models for Passive Microwave Soil Moisture Retrieval Using Data From ComRAD Ground-Based SMAP Simulator," in *IEEE Journal of Selected Topics in Applied Earth Observations and Remote Sensing*, vol. 8, no. 9, pp. 4345-4354, Sept. 2015, DOI: 10.1109/JSTARS.2014.2372031.

[3] D. Entekhabi *et al*., "The Soil Moisture Active Passive (SMAP) Mission," in *Proceedings of the IEEE*, vol. 98, no. 5, pp. 704-716, May 2010, DOI: 10.1109/JPROC.2010.2043918.

[4] B. J. Choudhury, T. J. Schmugge, A. Chang and R. W. Newton, "Effect of surface roughness on the microwave emission from soils," in *J. Geophys. Res*., 84(C9), 5699–5706, 1979, DOI: 10.1029/JC084iC09p05699.

[5] P. Marzahn, D. Rieke-Zapp, and R. Ludwig, "Assessment of soil surface roughness statistics for microwave remote sensing applications using a simple photogrammetric acquisition system," in *ISPRS Journal of Photogrammetry and Remote Sensing*, vol. 72, pp. 80-89, 2012, DOI: 10.1016/j.isprsjprs.2012.06.005.

[6] D. Rieke-Zapp, H. Wegmann, F. Santel, M.A. Nearing, "Digital photogrammetry for measuring soil surface roughness," in *2001 Proceedings of the American Society of Photogrammetry & Remote Sensing*. Presented at Gateway to the New Millennium. St. Louis, Missouri, USA. 23.-27.04.2001.

[7] E. G. Njoku *et al*., "Observations of soil moisture using a passive and active low-frequency microwave airborne sensor during SGP99," in *IEEE Transactions on Geoscience and Remote Sensing*, vol. 40, no. 12, pp. 2659-2673, Dec. 2002, DOI: 10.1109/TGRS.2002.807008.

[8] F.T. Ulaby, D.G. Long, W. Blackwell, Ch. Elachi, A. Fung, C. Ruf, K. Sarabandi, H. Zebker and J.J. van Zyl, *Microwave radar and radiometric remote sensing*. University of Michigan. Press Ann Arbor, 2014.

[9] P. S. Narvekar, D. Entekhabi, S. Kim and E. G. Njoku, "Soil Moisture Retrieval Using L-Band Radar Observations," in *IEEE Transactions on Geoscience and Remote Sensing*, vol. 53, no. 6, pp. 3492-3506, June 2015, DOI: 10.1109/TGRS.2014.2377714.

[10] N. N. Das, D. Entekhabi and E. G. Njoku, "An Algorithm for Merging SMAP Radiometer and Radar Data for High-Resolution Soil-Moisture Retrieval," in *IEEE Transactions on Geoscience and Remote Sensing*, vol. 49, no. 5, pp. 1504-1512, May 2011, DOI: 10.1109/TGRS.2010.2089526.

[11] J., Shi, J., Wang, A. Y. Hsu, P. E. O'Neill and E. T. Engman, "Estimation of bare surface soil moisture and surface roughness parameter using L-band SAR image data," in *IEEE Transactions on Geoscience and Remote Sensing*, vol. 35, no. 5, pp. 1254-1266, Sept. 1997, DOI: 10.1109/36.628792.

[12] Y. Oh, K. Sarabandi and F. T. Ulaby, "An empirical model and an inversion technique for radar scattering from bare soil surfaces," in *IEEE Transactions on Geoscience and Remote Sensing*, vol. 30, no. 2, pp. 370-381, March 1992, DOI: 10.1109/36.134086.

[13] M. C. Dobson and F. T. Ulaby, "Preliminaly Evaluation of the SIR-B Response to Soil Moisture, Surface Roughness, and Crop Canopy Cover," in *IEEE Transactions on Geoscience and Remote Sensing*, vol. GE-24, no. 4, pp. 517-526, July 1986, DOI: 10.1109/TGRS.1986.289666.

[14] U. Narayan, V. Lakshmi and E. Njoku, "Retrieval of Soil Moisture from Passive and Active L/S Band Sensor (PALS) Observations During the Soil Moisture Experiment in 2002 (SMEX02)," in *Remote Sens. Env*., 92, 483-496, 2004, DOI: 10.1016/j.rse.2004.05.018.

[15] M. Piles, D. Entekhabi and A. Camps, "A Change Detection Algorithm for Retrieving High-Resolution Soil Moisture From SMAP Radar and Radiometer Observations," in *IEEE Transactions on Geoscience and Remote Sensing*, vol. 47, no. 12, pp. 4125-4131, Dec. 2009, DOI: 10.1109/TGRS.2009.2022088.

[16] N. N. Das, D. Entekhabi, E. G. Njoku, J. J. C. Shi, J. T. Johnson and A. Colliander, "Tests of the SMAP Combined Radar and Radiometer Algorithm Using Airborne Field Campaign Observations and Simulated Data," in *IEEE Transactions on Geoscience and Remote Sensing*, vol. 52, no. 4, pp. 2018-2028, April 2014, DOI: 10.1109/TGRS.2013.2257605.

[17] S. Saatchi, E. Njoku, U. Wegmüller, "Synergism of active and passive microwave data for estimating bare soil surface moisture", in *ESA/NASA Int. Workshop Passive Microwave Remote Sens. Res. Related to Land-atmosphere*. Interactions, Saint-Lary, France, Jan. 11-15 1993, pp. 205-224.

[18] F. T. Ulaby, R. K. Moore and A. K. Fung, Microwave remote sensing: Active and passive. Volume 2-Radar remote sensing and surface scattering and emission theory. Boston, USA, Artech House, 1982.

[19] J.-P. Wigneron, Y. Kerr, P. Waldteufel, K. Saleh, M.-J. Escorihuela, P. Richaume, P. Ferrazzoli, P. de Rosnay, R. Gurney, J.-C. Calvet, J.P. Grant, M. Guglielmetti, B. Hornbuckle, C. Mätzler, T. Pellarin and M. Schwank, "L-band Microwave Emission of the Biosphere (L-MEB) Model: Description and calibration against experimental data sets over crop fields," in *Remote Sensing of Environment*, vol. 107, issue 4, pp. 639-655, 2007, DOI: 10.1016/j.rse.2006.10.014.

[20] J.-P. Wigneron, T.J. Jackson, P. O'Neill, G. De Lannoy, P. de Rosnay, J.P. Walker, P. Ferrazzoli, V. Mironov, S. Bircher, J.P. Grant, M. Kurum, M. Schwank, J. Munoz-Sabater, N. Das, A. Royer, A. Al-Yaari, A. Al Bitar, R. Fernandez-Moran, H. Lawrence, A. Mialon, M. Parrens, P. Richaume, S. Delwart and Y. Kerr, "Modelling the passive microwave signature from land surfaces: A review of recent results and application to the L-band SMOS & SMAP soil moisture retrieval algorithms," in *Remote Sensing of Environment*, vol. 192, pp. 238-262, 2017, DOI: 10.1016/j.rse.2017.01.024.

[21] N.E. Verhoest, H. Lievens, W. Wagner, J. Álvarez-Mozos, M.S. Moran, F. Mattia, "On the Soil Roughness Parameterization Problem in Soil Moisture Retrieval of Bare Surfaces from Synthetic Aperture Radar," in *Sensors*, vol. 8, pp. 4213-4248, 2008, DOI: 10.3390/s8074213.

[22] U. Wegmuller and C. Matzler, "Rough bare soil reflectivity model," in *IEEE Transactions on Geoscience and Remote Sensing*, vol. 37, no. 3, pp. 1391-1395, May 1999, DOI: 10.1109/36.763303.

[23] T. Mo, B.J. Choudhury, T.J. Schmugge, J.R. Wang and T.J. Jackson, "A Model for Microwave Emission from Vegetation-Covered Soils," in *Journal of Geophysical Research*, vol. 87, pp. 229-237, 1982, DOI: 10.1029/JC087iC13p11229.

[24] J. R. Wang, and B. J. Choudhury, "Remote sensing of soil moisture content over bare field at 1.4 GHz frequency," in *J. Geophys. Res*., 86(C6), 5277–5282, 1981, DOI: 10.1029/JC086iC06p05277.

[25] H. Lawrence, J. Wigneron, F. Demontoux, A. Mialon and Y. H. Kerr, "Evaluating the Semiempirical H - Q Model Used to Calculate the L-Band Emissivity of a Rough Bare Soil," in *IEEE Transactions on Geoscience and Remote Sensing*, vol. 51, no. 7, pp. 4075-4084, July 2013, DOI: 10.1109/TGRS.2012.2226995.

[26] T. Mo and T. J. Schmugge, "A Parameterization of the Effect of Surface Roughness on Microwave Emission," in *IEEE Transactions on Geoscience and Remote Sensing*, vol. GE-25, no. 4, pp. 481-486, July 1987, DOI: 10.1109/TGRS.1987.289860.

[27] J. Álvarez-Mozos, N.E Verhoest, A. Larrañaga, J. Casalí, M. González-Audícana, "Influence of Surface Roughness Spatial Variability and Temporal Dynamics on the Retrieval of Soil Moisture from SAR

Observations," in *Sensors*, 9, pp. 463-489, 2009, DOI: 10.3390/s90100463.

[28] Fung, A.K. *Microwave scattering and emission models and their applications*; Artech House: Boston, MA, 1994.

[29] R. Akbar, M. H. Cosh, P. E. O'Neill, D. Entekhabi and M. Moghaddam, "Combined Radar–Radiometer Surface Soil Moisture and Roughness Estimation," in *IEEE Transactions on Geoscience and Remote Sensing*, vol. 55, no. 7, pp. 4098-4110, July 2017, DOI: 10.1109/TGRS.2017.2688403.

[30] D. Entekhabi, S. Yueh, P. O'Neill, K.H. Kellogg and E. Al, *SMAP Handbook*, 2014.

[31] SMAP data 2015 (NASA). Dataset: SMAP_L1B_S0_LoRes_V2. Retrieved from ASF DAAC 7 December 2015. DOI: 10.5067/J4SZZV52B88J.

[32] S. Chan, E.G. Njoku and A. Colliander, *SMAP L1C Radiometer Half-orbit 36 km EASE-grid Brightness Temperatures, Version 3*. Global Projection. NASA National Snow and Ice Data Center Distributed Active Archive Center, Boulder, Colorado USA, 2016, DOI: 10.5067/E51BSP6V3KP7. [08/30/2017].

[33] P.E. O'Neill *et al*., *SMAP L3 Radiometer Global Daily 36 km EASE-Grid Soil Moisture, Version 4*. Global Projection. NASA National Snow and Ice Data Center Distributed Active Archive Center, Boulder, Colorado USA, 2016, DOI: 10.5067/OBBHQ5W22HME. [08/30/2017].

[34] D. Entekhabi, N. N. Das, E.G. Njoku, S. Yueh, J.T. Johnson and J. Shi, Soil Moisture Active Passive (SMAP). Algorithm Theoretical Basis Document L2 & L3 Radar/Radiometer Soil Moisture (Active/Passive) Data Products. Revision A. Jet Propulsion Lab., California Inst. Technol., Pasadena, CA, USA, 2014.

[35] A.G. Konings, M. Piles, N. N. Das and D. Entekhabi, "L-band vegetation optical depth and effective scattering albedo estimation from SMAP," in *Remote Sensing of Environment*, vol. 198, pp. 460-470, 2017, DOI: 10.1016/j.rse.2017.06.037.

[36] X. Xu *et al.*, *SMAP L3 Radiometer Northern Hemisphere Daily 36 km EASE-Grid Freeze/Thaw State, Version 1*. Global Projection. Boulder, Colorado USA. NASA National Snow and Ice Data Center Distributed Active Archive Center, 2016, DOI: 10.5067/RDEJQEETCNWV. [08/30/17].

[37] T.J. Jackson and T.J. Schmugge, "Vegetation Effects on the Microwave Emission of Soils," in *Remote Sensing of Environment*, 36, pp. 203-212, 1991, DOI: 10.1016/0034-4257(91)90057-D.

[38] Jagdhuber, T. *et al.*, "Physics-Based Modeling of Active and Passive Microwave Covariations Over Vegetated Surfaces," in *IEEE Transactions on Geoscience and Remote Sensing*, vol. 57, issue 2, pp. 788-802, 2018, DOI: 10.1109/TGRS.2018.2860630.

[39] K. S. Chen, Tzong-Dar Wu, Leung Tsang, Qin Li, Jiancheng Shi and A. K. Fung, "Emission of rough surfaces calculated by the integral equation method with comparison to three-dimensional moment method simulations," in *IEEE Transactions on Geoscience and Remote Sensing*, vol. 41, no. 1, pp. 90-101, Jan. 2003, DOI: 10.1109/TGRS.2002.807587.

[40] Fung, A.K. *et al.*, "An Improved IEM Model for Bistatic Scattering From Rough Surfaces," in *Journal of Electromagnetic Waves and Applications*, *16*, pp. 689–702, 2002. DOI: 10.1163/156939302X01119.

[41] L. Tsang *et al*., "Active and Passive Vegetated Surface Models With Rough Surface Boundary Conditions From NMM3D," in *IEEE Journal of Selected Topics in Applied Earth Observations and Remote Sensing*, vol. 6, no. 3, pp. 1698-1709, June 2013, DOI: 10.1109/JSTARS.2013.2257694.

[42] C.A. Mack, "Analytic form for the power spectral density in one, two, and three dimensions," in *J. Micro/Nanolith, MEMS MOEMS*, 10(4), Oct. 2011, DOI: 10.1117/1.3663567.

[43] J.A. Ogilvy and J.R. Foster, "Rough surfaces: gaussian or exponential statistics?" in *J. Phys. D: Appl. Phys*, vol.. 22, pp. 1243-1251, 1989, DOI: 10.1088/0022-3727/22/9/001.

[44] Agricultural Institute, Bureau of Meteorology, Australian Government: http://www.bom.gov.au/climate/data/index.shtml?bookmark=136 [07/27/2018].

[45] N.N. Das, *Ancillary Data Report: Soil Attributes*. Jet Propuls. Lab. Calif. Inst. Technol., JPL D-53058, 2013.

[46] W.R. Wieder, J. Boehnert, G.B. Bonan, and M. Langseth, "Regridded Harmonized World Soil Database v1.2. Data set. Available online [http://daac.ornl.gov] from Oak Ridge National Laboratory Distributed Active Archive Center, Oak Ridge, Tennessee, USA", 2014, DOI: http://dx.doi.org/10.3334/ORNLDAAC/1247 .

[47] R. Bindlish, T. Jackson, R. Sun, M. Cosh, S. Yueh and S. Dinardo, "Combined Passive and Active Microwave Observations of Soil Moisture During CLASIC," in *IEEE Geoscience and Remote Sensing Letters*, vol. 6, no. 4, pp. 644-648, Oct. 2009, DOI: 10.1109/LGRS.2009.2028441.

[48] D. M. Le Vine, G. S. E. Lagerloef, F. R. Colomb, S. H. Yueh and F. A. Pellerano, "Aquarius: An Instrument to Monitor Sea Surface Salinity From Space," in *IEEE Transactions on Geoscience and Remote Sensing*, vol. 45, no. 7, pp. 2040-2050, July 2007, DOI: 10.1109/TGRS.2007.898092.

[49] T. Jagdhuber *et al*., "Physically-based retrieval of SMAP active-passive measurements covariation and vegetation structure parameters," *2016 IEEE International Geoscience and Remote Sensing Symposium (IGARSS)*, Beijing, 2016, pp. 3078-3081, DOI: 10.1109/IGARSS.2016.7729796.

[50] V. Gupta and R. Jangid, "Microwave response of rough surfaces with autocorrelation functions, RMS heights and correlation lengths using active remote sensing," in *Indian Journal of Radio and Space Physics*, 40, pp. 137–146, 2011.

[51] N. Baghdadi, M. Zribi, S. Paloscia, N. Verhoest, H. Lievens, F. Baup and F. Mattia, "Semi-Empirical Calibration of the Integral Equation Model for Co-Polarized L-Band Backscattering," in *Remote Sensing*, 7, pp. 13626–13640, 2015, DOI:10.3390/rs71013626.

[52] J. Peng, A. Loew, O. Merlin and N.E.C. Verhoest, "A review of spatial downscaling of satellite remotely sensed soil moisture," in *Rev. Geophys*., 55, pp. 1-26, 2017, DOI: 10.1002/2016RG000543.

[53] L. Zhixiong, C. Nan, U.D. Perdok and W.B. Hoogmoed, "Characterisation of Soil Profile Roughness," in *Biosystems Engineering*, 91, pp. 369–377, 2005, DOI: 10.1016/j.biosystemseng.2005.04.004.

[54] M. Kurum, P.E. O'Neill, R.H. Lang, A.T. Joseph, M.H. Cosh, T.J. Jackson, "Effective tree scattering and opacity at L-band," in *Remote Sensing of Environment*, vol. 118, pp. 1-9, 2012, DOI: 10.1016/j.rse.2011.10.024.

[55] D. van der Wal, P. M. J. Herman and A. Wielemaker-van den Dool, "Characterisation of surface roughness and sediment texture of intertidal flats using ERS SAR imagery," in *Remote Sensing of Environment*, vol. 98, issue 1, pp. 96-109, 2005, DOI: 10.1016/j.rse.2005.06.004.

Anke Fluhrer (S'17–M'18) received the B.S. degree in geography from the Julius-Maximilians-University Würzburg, Würzburg, Germany, in 2014, and the M.S. degree in physical geography from the Friedrich-Alexander University Erlangen-Nuernberg, Erlangen, Germany, in 2018. She is currently a Research Associate with the prospect of a Ph.D. at the German Aerospace Center (DLR), Oberpfaffenhofen, Germany. Her research interests include terrestrial remote sensing, satellite image processing, and data assimilation.

Thomas Jagdhuber (S'08–M'12–SM'19) received his Diploma degree (with honors) in physical geography, physics, remote sensing and geoinformatics from Ludwig Maximilian University of Munich, Munich, Germany, in 2006 and his Ph.D degree (with honors) in hydrology from the Faculty of Science at the University of Potsdam, Potsdam, Germany, in 2012. His main research interests include physics-based multi-sensor data integration with focus on active and passive microwave interaction theory and on polarimetric techniques for hydrological, cryospheric and agricultural parameter modeling and estimation. Since 2007 he is affiliated with the Microwaves and Radar Institute (HR) of the German Aerospace Center (DLR). In 2014 he was honored with the DLR Science Award for his research on polarimetric SAR decomposition techniques. From 2014 through 2019, he was a yearly visiting scientist at the Massachusetts Institute of Technology (MIT), Boston, USA, contributing to the preparation and continuation of the SMAP and SMAP/Sentinel-1 missions. Together with Prof. Dr. Entekhabi (MIT), he was awarded with the MIT-MISTI grant for global water cycle and environmental monitoring using active and passive satellite-based microwave instruments. In addition, Dr. Jagdhuber serves as a lecturer for the University of Jena and the University of Augsburg as well as a reviewer for several international journals and conference boards.

Ruzbeh Akbar (S'05–M'13) received the B.S. (*summa cum laude*) degree from The George Washington University, Washington, DC, USA, in 2009, the M.S. degree from the University of Michigan, Ann Arbor, MI, USA, in 2011, and the Ph.D. degree from the University of Southern California, Los Angeles, CA, USA, in 2016, all in electrical engineering. He is currently a Postdoctoral Research Associate with the Massachusetts Institute of Technology, Cambridge, MA, USA. His research interests include terrestrial remote sensing, electromagnetic theory, and hydrology. Dr. Akbar was a recipient of the NASA Earth and Space Science Fellowship from 2010 to 2014.

Peggy E. O'Neill (F'16) received the B.S. (*summa cum laude*) degree (Hons.) in geography from Northern Illinois University, DeKalb, IL, USA, in 1976, and the M.A. degree in geography from the University of California at Santa Barbara, Santa Barbara, CA, USA, in 1979. She has done postgraduate research in civil and environmental engineering at Cornell University, Ithaca, NY, USA. Since 1980, she has been a Physical Scientist with the Hydrological Sciences Laboratory, NASA/Goddard Space Flight Center, Greenbelt, MD, USA, where she conducts research in soil moisture retrieval and land surface hydrology, primarily through microwave remote sensing techniques. She is currently the SMAP Deputy Project Scientist.

Dara Entekhabi (M'04–SM'09–F'15) received the B.S. and M.S. degrees from Clark University, Worcester, MA, USA, and the Ph.D. degree from the Massachusetts Institute of Technology (MIT), Cambridge, MA, USA, in 1990. He is currently a Professor with the Department of Civil and Environmental Engineering, MIT. He is also the Science Team Lead of the National Aeronautics and Space Administration's Soil Moisture Active and Passive (SMAP) Mission that was launched in 2015. His research interests include terrestrial remote sensing, data assimilation, and coupled land–atmosphere systems modeling. Dr. Entekhabi is a Fellow of the American Meteorological Society and the American Geophysical Union.